DOI: 10.1002/ejic.200700799

Intramolecular Host–Guest Dynamics of $FeCp(CO)_2X$ (X = I and CH_3) and $Mo_2Cp_2(CO)_6$ Included in β- or γ-Cyclodextrin

Silvio Aime,[a] Michele R. Chierotti,[a] Roberto Gobetto,*[a] Admir Masic,[a] Fabio Napolitano,[a] Holly C. Canuto,[b] and Stephen J. Heyes[b]

Keywords: Solid-state NMR spectroscopy / Anisotropy / Inclusion compounds / Cyclodextrins / Metal–carbonyl complexes / Molecular dynamics

Variable-temperature ^{13}C CPMAS NMR spectra of the metal–carbonyl complexes $FeCp(CO)_2X$ (where X = I, CH_3) and $Mo_2Cp_2(CO)_6$ included in β- or γ-cyclodextrin (CD) cavities were investigated in the temperature range 133 to 293 K. The motion of the guest molecule inside the CD can be detected by comparing these spectra with the static crystalline patterns of $FeCp(CO)_2I$ and $Mo_2Cp_2(CO)_6$. In the case of $FeCp(CO)_2CH_3$, solid-state plastic crystal behaviour is noted for the free guest; the molecular motion is further modified by inclusion within the CD cavity. The nature of the molecular motion found within the metal–carbonyl/CD adducts was shown to be dependent on the symmetry, size and orientation of the guest molecule within the host cavity. In the case of $Mo_2Cp_2(CO)_6$ included in γ-CD, the two $[MoCp(CO)_3]$ ends of the dimer may be considered as separate dynamic entities: one half of the moiety within the CD cavity exhibits a greater freedom of motion, whereas the other end of the dimer is anchored.

Introduction

Inclusion compounds based on the hydrophobic interaction of a guest molecule with α-, β- and γ- cyclodextrins (CDs) are under intense scrutiny in a number of fields, and as a result, several useful applications of inclusion compounds have become available.[1,2] A large variety of inorganic and organic "host–guest" molecules have been obtained by using CDs, and their water solubility, low toxicity and relatively low cost make them suitable for a wide range of applications in food technology,[3–5] drug delivery systems,[6–10] chemical sensors[11–13] and enzyme mimics.[14] Other important applications that have been suggested include enantiomeric enrichment, isomer separation, molecular recognition and removal of undesired compounds from industrial products.[1] It is therefore of interest to obtain the most detailed characterisation of such "host–guest" adducts, including in-depth knowledge of the dynamics of "host" species within the CD cavity.[15,16]

Until recently, studies into the dynamics of CD "host–guest" systems have been greatly limited, as interest has been mainly focused on the characterisation of the crystal structure; however, the ability of the CD cavity to lower the activation energy barriers between molecules in the solid state and hence facilitate molecular motions by decreasing interatomic forces among molecules has been recently highlighted.[17] Moreover, it was shown that the nature and the extent of internal motions are dependent on the interplay between the symmetry and the shape of the host and guest molecules.[18–21] We previously reported the inclusion of simple binary metal–carbonyl complexes such as $Fe(CO)_5$ and $Cr(CO)_6$ in β- and γ-CD cavities and their subsequent dynamics were assessed by using solid-state NMR spectroscopic techniques.[20] Interestingly for the highly symmetric $Fe(CO)_5$ and $Cr(CO)_6$ systems, the entire molecule undergoes fast isotropic motion inside the CD.[20] In the case of $Cr(CO)_3$(arene) compounds, fast carbonyl exchange was observed even at low temperatures, as the pseudo-octahedral structure of the organometallic complex allowed the $Cr(CO)_3$ moiety to rotate at an angle close to 54.7°.[21] Recently, variable temperature (VT) ^{13}C CPMAS NMR spectroscopic studies on $Fe_2Cp_2(CO)_4$ included in γ-CD showed that the microenvironment provided by the γ-CD cavity facilitated extensive rearrangements, which promoted distinct structural changes within the metal complexes such as *cis–trans* isomerisation.[22]

In the present study, we report some novel inclusion compounds of mono- and binuclear metal–carbonyl complexes of differing size and shape as guest molecules in CD. The dynamics of the guest molecule were studied by means of VT ^{13}C CPMAS NMR spectroscopy with the specific aim of determining how the interplay of the symmetry and shape of the guest molecule determines the extent of the angular motions.

---

[a] Dipartimento di Chimica IFM, Università di Torino,
Via P. Giuria 7, 10125 Torino, Italy
E-mail: roberto.gobetto@unito.it
[b] Inorganic Chemistry Laboratory, Department of Chemistry, University of Oxford,
South Parks Road, Oxford, OX1 3QR, UK
E-mail: hcc36@cam.ac.uk

Results and Discussions

$FeCp(CO)_2I$

The room-temperature ^{13}C CPMAS NMR spectrum of ^{13}CO-enriched $FeCp(CO)_2I$ (Figure 1, top) recorded at 10 kHz shows the presence of two narrow peaks at 211.3 and 81.3 ppm for the two CO groups and the Cp moiety, respectively. When the spinning rate was reduced to 2 kHz (Figure 1, bottom) the appearance of a larger spinning sideband (SSB) pattern allowed the calculation, by means of computer simulation,[23] of the chemical shift tensor components (δ_{11}, δ_{22} and δ_{33} with $\delta_{11} > \delta_{22} > \delta_{33}$) and the shielding anisotropy [defined as $\Delta\sigma = \sigma_{33} - (\sigma_{11} + \sigma_{22})/2$ with $\sigma_{11} \leq \sigma_{22} \leq \sigma_{33}$ and $\sigma_{ii} = -\delta_{ii}$], as reported in Table 1. The small size of the SSB pattern in the NMR spectrum confirmed that fast rotation of the Cp ring in the crystalline compound was possible, which gave rise to a low value for the shielding anisotropy ($\Delta\sigma$ = 86 ppm). In contrast, the large SSB manifold ($\Delta\sigma$ = 411 ppm) associated with the carbonyl moieties indicated the static nature of the CO ligands.[24] This situation, in which rotation of the ring is fast but the motion of the carbonyl groups is limited because of crystal-packing constraints, is characteristic of half-sandwich complexes at most instrumentally obtainable temperatures. A VT ^{13}C CPMAS NMR study in the range 153 to 493 K showed that the CO group remained static, as no changes were observed in either the SSB manifold or the peak shape.

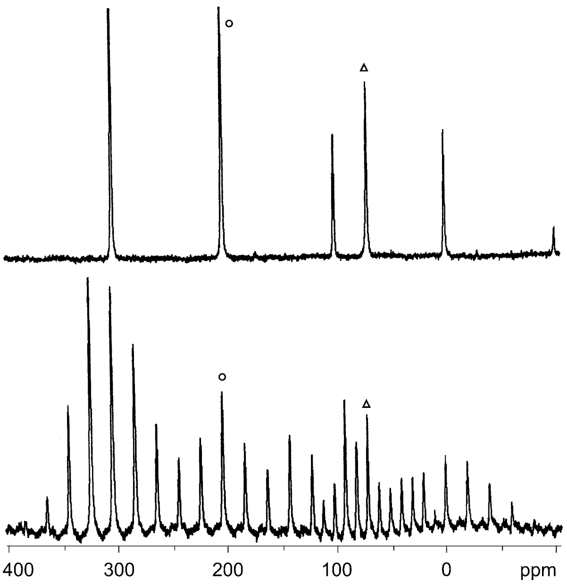

Figure 1. ^{13}C CPMAS NMR spectra of crystalline $FeCp(CO)_2I$ at 10 kHz (top) and 2 kHz (bottom) recorded at 100.64 MHz. The Cp and CO isotropic peaks are marked by a triangle (Δ) and empty dot (○), respectively.

Table 1. ^{13}C chemical shift tensor components (δ_{11}, δ_{22} and δ_{33} with $\delta_{11} > \delta_{22} > \delta_{33}$) and the shielding anisotropy [defined as $\Delta\sigma = \sigma_{33} - (\sigma_{11} + \sigma_{22})/2$ with $\sigma_{11} \leq \sigma_{22} \leq \sigma_{33}$ and $\sigma_{ii} = -\delta_{ii}$] for compounds $FeCp(CO)_2I$, $FeCp(CO)_2I$/β-CD, $FeCp(CO)_2CH_3$ and $FeCp(CO)_2CH_3$/β-CD.

Compound	δ_{iso} [ppm]	δ_{11} [ppm]	δ_{22} [ppm]	δ_{33} [ppm]	$\Delta\sigma$ [ppm]
$FeCp(CO)_2I$	221.3	348	348	–63	411
	81.3	110	110	24	87
$FeCp(CO)_2I$/β-CD	208.3	245	212	168	60
$FeCp(CO)_2CH_3$	221.3	344[a]	322[a]	–2[a]	335[a]
$FeCp(CO)_2CH_3$/β-CD	213.7 212.8	241	206	189	34

[a] These values were obtained from spectra recorded at 153 K.

The results from Figure 1 can be compared with the ^{13}C CPMAS NMR spectrum of $FeCp(CO)_2I$ in β-CD recorded at the same spinning rate of 10 kHz (Figure 2, top). The most prominent difference is the complete absence of an SSB pattern for the carbonyl resonance at δ = 208.3 ppm. When the spinning speed was reduced to 2 kHz (Figure 2, bottom) the appearance of a small, but significant, SSB manifold allowed the calculation of the chemical shift tensors and evaluation of a shielding anisotropy ($\Delta\sigma$ = 60 ppm) for the carbonyl peak (Table 1). No changes were observed in the SSB manifold in the VT NMR spectroscopic experiments over the range 153 to 493 K. The signals around 50–100 ppm belong to the CD and Cp carbon atoms (probably ca. 80 ppm).

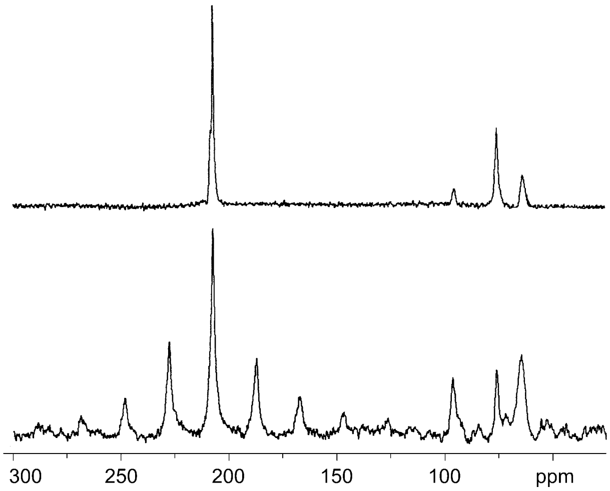

Figure 2. ^{13}C CPMAS NMR spectra of $FeCp(CO)_2I$ included in β-CD at 10 kHz (top) and 2 kHz (bottom) recorded at 100.64 MHz.

Upon formation of the inclusion complex, the overall molecular mobility was increased and parts of the molecule, which were previously reported as being static, gained mobility; this is shown by the reduced CSA values calculated for the ^{13}CO resonance. However, the dynamic process that occurred did not appear to completely average out the chemical shift anisotropy of the two CO groups. These results can be explained by the presence of fast molecular rotations of the entire molecule around a clearly defined axis, which would account for a reduction of the shielding anisotropy of the axial carbonyl group by a factor of ca.

0.15 (from 411 to 60 ppm). In fact, it is well known[25] that the anisotropy of mobile nuclei is reduced according to Equation (1)

$$\Delta\sigma' = \Delta\sigma(3\cos^2\beta - 1)/2 \qquad (1)$$

where $\Delta\sigma'$ is the effective shielding anisotropy, $\Delta\sigma$ is the anisotropy in the absence of mobility and β is the angle between the principal chemical shift tensor and the rotational axis. In this case, the principal axis of the chemical shift tensor for the CO groups would lie at an angle close to 49°, which would cause the entire molecule to precess around the *z* axis, as depicted in Scheme 1. We can also surmise the presence of precessional motion of the whole molecule about the main symmetry axis of the CD cavity. It is worth noting that such a motion has a very low-energy barrier, as it cannot be stopped even at the lowest attainable temperature (133 K).

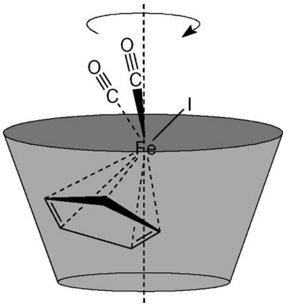

Scheme 1.

$FeCp(CO)_2CH_3$

The ^{13}C CPMAS NMR spectrum of a polycrystalline sample of $FeCp(CO)_2CH_3$ (Figure 3) is, at first, surprising because of its complete lack of CSA and its solution-like linewidths; peaks are observed at δ = 221.3, 89.9 and –18.0 ppm for the carbon atoms of the carbonyl group, the aromatic ring and the methyl group, respectively. When recorded under static conditions, the carbonyl peak linewidth is only ca. 250 Hz (Figure 3). Interestingly, the crystalline compound displays plastic, crystal-like behaviour at ambient temperature, as observed from the ^{13}C CPMAS NMR spectrum.

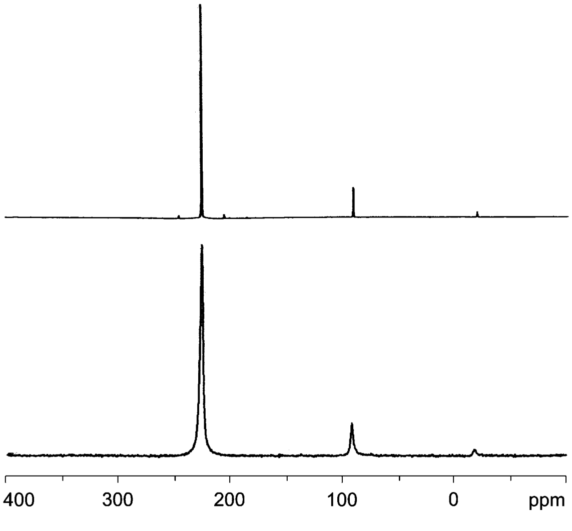

Figure 3. ^{13}C CPMAS NMR spectra of crystalline $FeCp(CO)_2CH_3$ with a spinning speed of 10 kHz (top) and without spinning the sample (bottom) recorded at 100.64 MHz.

As the temperature was lowered, molecular motion decreased, and the corresponding effects were detected in the SSB pattern of the individual resonances (Figure 4); however, a static situation was reached at 263 K as determined by the CSA value for the carbonyl peak ($\Delta\sigma$ = 335 ppm).

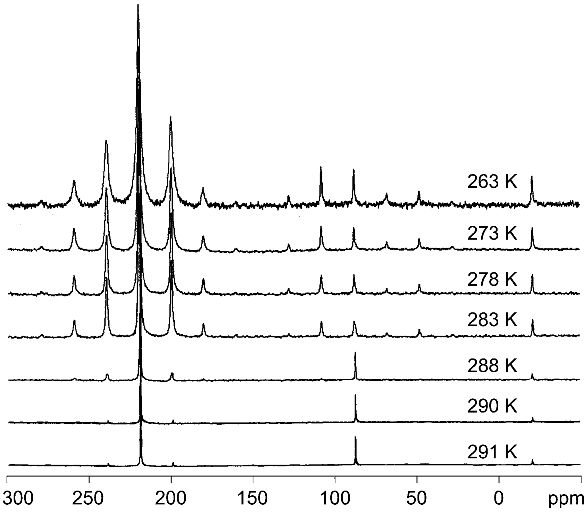

Figure 4. VT (291–263 K) ^{13}C CPMAS NMR spectra of crystalline $FeCp(CO)_2CH_3$ recorded at 100.64 MHz with a spinning speed of 10 kHz.

The ^{13}C CPMAS NMR spectrum of $FeCp(CO)_2CH_3$ included in β-CD at room temperature (Figure 5) is similar to the spectra obtained for $FeCp(CO)_2I$ in β-CD, which is discussed above. At room temperature, the spectrum recorded at 10 kHz shows two equally intense carbonyl reso-

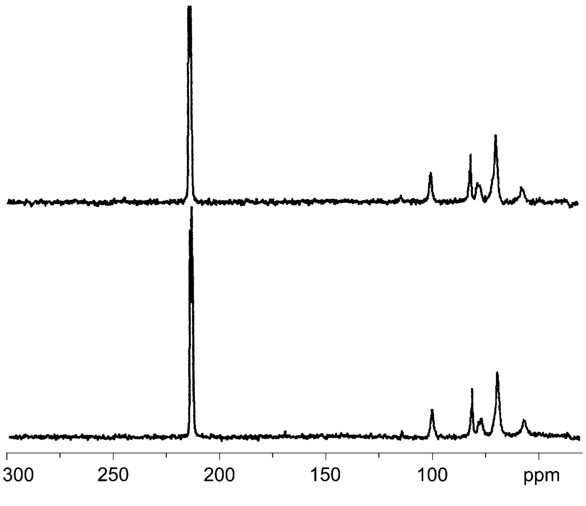

Figure 5. ^{13}C CPMAS NMR spectra of $FeCp(CO)_2CH_3$ included in β-CD at 143 (top) and 298 K (bottom) recorded at 100.64 MHz with a spinning speed of 10 kHz.

nances at δ = 213.7 and 212.8 ppm, which probably indicates that the two ligands are in different environments. When the spinning speed was reduced to 2 kHz, a SSB pattern was observed. The average value of the shielding anisotropy for the two peaks is $\Delta\sigma$ = 34 ppm. Once again, no change was observed when the temperature was decreased to 143 K (Figure 5). When $FeCp(CO)_2CH_3$ is included in β-CD, its dynamic behaviour is quite similar to that found for $FeCp(CO)_2I$, which is discussed above. Upon formation of the inclusion compound, the two carbonyl groups are no longer equivalent, which leads to different isotropic chemical shifts. We obtained a β angle of 51° by applying Equation (1) to the shielding-anisotropy value, which was calculated from analysis of the SSB intensities.

$Mo_2Cp_2(CO)_6$

At room temperature, the ^{13}C CPMAS NMR spectrum (Figure 6) obtained for a polycrystalline sample of $Mo_2Cp_2(CO)_6$ shows three carbonyl resonances with roughly equally intensities at δ = 234.1, 227.2 and 225.5 ppm and a cyclopentadienyl peak at δ = 91.3 ppm. The SSB manifold present for each carbonyl resonance was analysed; the associated chemical shift anisotropy values (Table 1) clearly indicate the static nature of the complex.

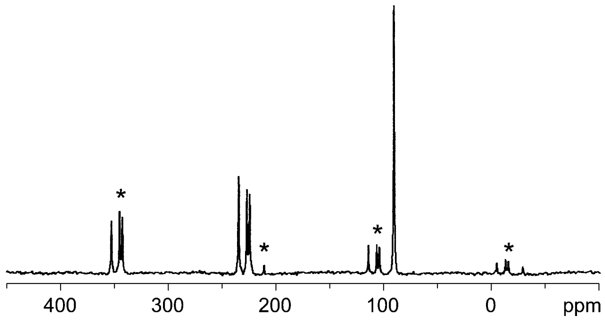

Figure 6. ^{13}C CPMAS NMR spectra of crystalline $Mo_2Cp_2(CO)_6$ recorded at 100.64 MHz with a spinning speed of 10 kHz. The spinning sidebands are marked with an asterisk (*).

The ^{13}C CPMAS NMR spectrum of the metal–carbonyl/γ-CD adduct at ambient temperature (Figure 7) shows subtle, yet important, differences in comparison to the analogous spectrum recorded for the pure compound. It is worth noting that the SSB pattern reveals greater peak resolution relative to that observed in the isotropic region alone. Close inspection of the isotropic-carbonyl region of the inclusion compound (Figure 7, inset) shows the presence of two distinct peaks at δ = 234.5 and 225.3 ppm (relative intensity ratio ca. 1:2) with shoulders at 235.2, 227.1 and 228.0 ppm. As the temperature was lowered to 133 K, there was a gradual appearance of at least six new peaks in the isotropic region at 235.2, 234.5, 228.1, 227.1, 225.3 and 224.4 ppm (Figure 8).

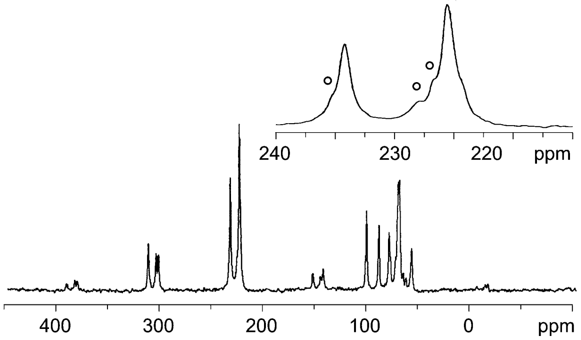

Figure 7. ^{13}C CPMAS NMR spectra of $Mo_2Cp_2(CO)_6$ in γ-CD recorded at 100.64 MHz with a spinning speed of 10 kHz. In the inset the carbonyl region is shown with the shoulders at 235.2, 227.1 and 228.0 ppm marked with a circle (○).

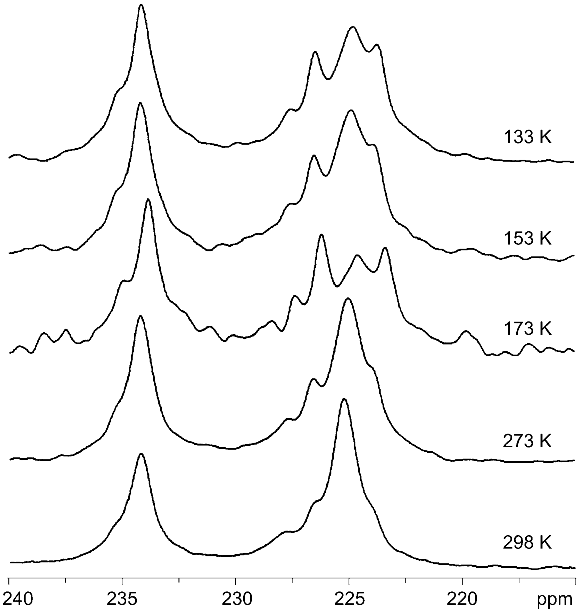

Figure 8. VT (298–133 K) ^{13}C CPMAS NMR spectra (carbonyl region) of $Mo_2Cp_2(CO)_6$ in γ-CD recorded at 100.64 MHz with a spinning speed of 10 kHz.

Ostensibly, the ambient-temperature ^{13}C CPMAS NMR spectrum of $Mo_2Cp_2(CO)_6$ included in γ-CD (at a spinning rate of 10 kHz) differs slightly from the spectrum recorded for the pure compound by the presence of only two main peaks and three shoulders in the isotropic region; moreover, the same region became more complex as the temperature was decreased and several resonances (up to six) became clearly detectable. The SSB manifold that appeared when the temperature was decreased also displays peculiar features. At room temperature, the relative intensities of the peaks in each SSB do not reflect the intensities of the absorptions of the central band, as these are very similar to those found for the polycrystalline sample; however, the overall intensity of the SSB increases as the temperature decreases (and the isotropic region becomes more complex). We suggest that the observed behaviour can be attributed to the presence of different motional regimes for each of the two halves of the $Mo_2Cp_2(CO)_6$ complex. Although it is not possible to confirm the type of intermolecular interactions involved in the crystal packing arrangement, the observed behaviour is in agreement with a model in which half of the $Mo_2Cp_2(CO)_6$ complex is located inside the γ-CD cavity, where fast motion at room temperature is possible, whereas the other half of the $MoCp(CO)_3$ complex is located outside the CD cavity, where motion is not possible owing to packing constraints (Scheme 2). By decreasing the temperature, the rotation inside the cavity is slowed and more resonances become detectable in the centre band, which thus increases the SSB intensities. In most cases, it is very difficult to obtain high-quality single crystals from CD inclusion compounds formed with metal–organic complexes. This prevents the use of X-ray analysis to study the orientation of CDs and thus the possible binding modes for the intermolecular interactions of the $MoCp(CO)_3$ unit outside the cavity.

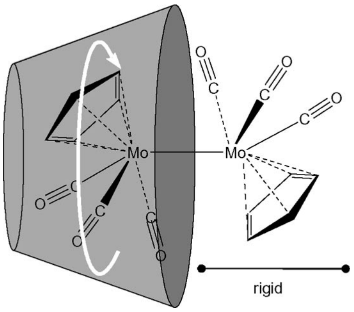

Scheme 2.

Conclusions

The supramolecular chemistry and molecular dynamics of metal–carbonyl/CD adducts were elucidated by solid-state NMR spectroscopic techniques. Information on the guest dynamics within the supramolecular cavity was evidenced by comparison of the CSA values recorded for the crystalline and inclusion compounds. The possible degree of symmetry, molecular size and the type, number and positioning of any functional groups associated with the organometallic guest complex are shown to determine the extent of the dynamics. This allows speculation as to the possible orientation of the guest within the host, which is often not available from single-crystal X-ray diffraction studies.

Experimental Section

General Remarks: $FeCp(CO)_2I$[26] and $FeCp(CO)_2CH_3$[26] were prepared according to published procedures.[23] $Mo_2Cp_2(CO)_6$ and γ-CD were used as supplied by Aldrich. All solvents were purified by standard techniques.[27]

Preparation of the CD Inclusion Compounds: The "host–guest" inclusion compounds were prepared following the method originally reported by Harada et al.[28] for ferrocene in γ-cyclodextrin. The appropriate metal–carbonyl complex was added to a saturated solution of γ-CD in distilled water and maintained at 60 °C for 3 h. The metal complex/cyclodextrin molar ratio was 1:1. The precipitate was collected by centrifugation, washed with aliquots of distilled water to eliminate any free cyclodextrin and then with benzene to remove any free organometallic compound. The elemental analysis was performed at the Analytical Service of the Inorganic Chemistry Laboratory, University of Oxford by using combustion for C and H and ICP-AES for Mo. It was shown that the inclusion compounds had a 1:1 cyclodextrin to metal–carbonyl complex ratio.

$(\eta^5\text{-}C_5H_5)Fe(CO)_2I$ in β-CD: To a stirred saturated solution of β-CD (0.3353 g, 0.25 mmol) in distilled water was added $(\eta^5\text{-}C_5H_5)Fe(CO)_2I$ (0.151 g, 1.5 10^{-4} mol). The resulting solution was stirred constantly by using a magnetic stirrer and kept at a constant temperature of 60 °C for 2.5 h. The formation of a grey precipitate indicated that inclusion had taken place. The precipitated intercalated compound was centrifuged to separate it from the aqueous solution. The solid was washed with distilled water (3 × 5 mL) to assure removal of any unreacted β-CD and with benzene (3 × 5 mL) to remove any remaining starting organometallic complex. A final washing with distilled water afforded the product (0.1311 g, 0.09 mmol, 75% yield) as a pale-grey powder.

$(\eta^5\text{-}C_5H_5)Fe(CO)_2CH_3$: To a round-bottomed flask flushed with nitrogen was added mercury (5 g) together with small portions of metallic sodium (320 mg, 13.9 mmol). As the amalgam started to cool and solidify, dry tetrahydrofuran (2.8 mL) and a solution of cyclopentadienyl irondicarbonyl dimer (500 mg, 1.141 mmol) in dry tetrahydrofuran (2.8 mL) were added. The overall solution was sealed and stirred overnight at room temperature. When the reaction was complete, iodomethane (1.24 mL, 19.9 mmol) was added dropwise by syringe over a 30 min period. The mixture was stirred in a sand bath for 2–3 h at 40 °C. The solvent was then removed, and the resulting product was sublimed at 50 °C under vacuum onto a water-cooled probe.

$(\eta^5\text{-}C_5H_5)Fe(CO)_2CH_3$ in β-CD: To a stirred saturated solution of β-CD (0.3353 g, 0.25 mmol) in distilled water was added $(\eta^5\text{-}C_5H_5)Fe(CO)_2CH_3$ (0.151 g, 1.5 10^{-4} mol). The resulting solution was stirred constantly by using a magnetic stirrer and kept at a constant temperature of 60 °C for 2.5 h. The formation of an orange precipitate indicated that inclusion had taken place. The intercalated product was purified by a procedure analogous to that described above for the iodine complex. The product (0.166 g, 1.2 10^{-1} mmol, 80% yield) was isolated as a pale-orange powder.

$Mo_2Cp_2(CO)_6$ in γ-CD: To a stirred saturated solution of γ-CD (0.605 g, 0.47 mmol) in distilled water was added $Mo_2Cp_2(CO)_6$ (0.114 g, 2.3 10^{-4} mol). The resulting solution was stirred constantly by using a magnetic stirrer and kept at a constant temperature of 60 °C for 8 h. The formation of a pale-pink precipitate indicated that inclusion had taken place. The intercalated product was purified by a procedure analogous to that described above for the iodine complex. The desired product (0.230 g, 1.63×10^{-4} mmol, 70% yield) was isolated as a pale-pink powder.

^{13}CO Enrichment of the $Fe(CO)_2X$ Group: The $Fe(CO)_2X$ group in all the iron compounds considered was enriched by treating it with a hexane solution of the ^{13}CO-enriched cyclopentadienyl irondicarbonyl dimer under 1 atm of ^{13}CO (99% enriched) for 48 h.[29]

Solid-State NMR Measurements: ^{13}C CPMAS NMR spectra were acquired with a Chemagnetics CMX Infinity 400 (9.4 T) instrument operating at 100.64 MHz for the ^{13}C nucleus. A standard cross-polarisation (CP) sequence was used for all acquisitions. Cylindrical 5-mm o.d. zirconia rotors with a sample volume of 120 µL were employed. For all samples, the magic angle was carefully adjusted from the ^{79}Br spectrum of KBr by minimising the linewidth of the spinning sideband satellite transitions. The principal components of the chemical shift tensors were extracted by computer simulation (HBA-graphical Herzfeld–Berger analysis written by K.

Eichele, R. E. Wasylishen, Dalhousie University, 2001) of the spinning sideband patterns obtained at low speed by using the algorithm developed by Herzfeld and Berger. The errors in the evaluation of the chemical shift tensor are less than 4 ppm as evaluated by repetition of the calculation at different spinning speeds.

---

[1] a) J. Szejtli, *Cyclodextrins and Their Inclusion Complexes,* Akadémiai Kiadó, Budapest, **1982**; b) F. Hapiot, S. Tilloy, E. Monflier, *Chem. Rev.* **2006**, *106*, 767–781.
[2] J. Szejtli, *Chem. Rev.* **1998**, *98*, 1743–1753.
[3] B. R. Bhandari, B. R. Darcy, *Food Aust.* **1996**, *48*, 547–551.
[4] F. Shahidi, X. Q. Han, *Crit. Rev. Food Sci. Nutr.* **1993**, *33*, 501–547.
[5] L. Szente, J. Szejtli, *Trends Food Sci. Technol.* **2004**, *15*, 137–142.
[6] A. T. Florence, P. U. Jani, *Drug Safety* **1994**, *10*, 233–266.
[7] T. Loftsson, M. Masson, *Int. J. Pharm.* **2001**, *225*, 15–30.
[8] B. J. Ravoo, *J. Controlled Release* **2001**, *72*, 254–256.
[9] K. Uekama, F. Hirayama, T. Irie, *Chem. Rev.* **1998**, *98*, 2045–2076.
[10] T. Loftsson, D. Duchêne, *Int. J. Pharm.* **2007**, *329*, 1–11.
[11] F. L. Dickert, A. Haunschild, *Adv. Mater.* **1993**, *5*, 887–895.
[12] B. Swanson, S. Johnson, J. Shi, X. Yang, *ACS Symp. Ser.* **1998**, *690*, 130–138.
[13] J. Yang, S.-C. Liang, *Anal. Chim. Acta* **2005**, *537*, 385–392.
[14] A. J. Kirby, *Angew. Chem. Int. Ed. Engl.* **1996**, *35*, 707–724 and references cited therein.
[15] W. Saenger, J. Jacob, K. Gessler, T. Steiner, D. Hoffmann, H. Sanbe, K. Koizumi, S. M. Smith, T. Takata, *Chem. Rev.* **1998**, *98*, 1787–1802.
[16] K. Harata, *Chem. Rev.* **1998**, *98*, 1803–1827.
[17] E. B. Brouwer, G. D. Enright, C. I. Ratcliffe, G. A. Facey, J. A. Ripmeester, *J. Phys. Chem. B* **1999**, *103*, 10604–10616.
[18] E. B. Brouwer, G. D. Enright, J. A. Ripmeester, *J. Am. Chem. Soc.* **1997**, *119*, 5404–5412.
[19] J. L. Atwood, L. J. Barbour, P. J. Nichols, C. L. Raston, C. A. Sandoval, *Chem. Eur. J.* **1999**, *5*, 990–996.
[20] H. C. Canuto, S. J. Heyes, S. Aime, R. Gobetto, F. Napolitano, *J. Chem. Soc. Dalton Trans.* **2000**, 4075–4077.
[21] S. Aime, H. C. Canuto, R. Gobetto, F. Napolitano, *Chem. Commun.* **1999**, 281–282.
[22] H. C. Canuto, A. Masic, N. Rees, S. J. Heyes, R. Gobetto, S. Aime, *Organometallics* **2006**, *25*, 2248–2252.
[23] J. Herzfeld, A. E. Berger, *J. Chem. Phys.* **1980**, *73*, 6021–6030.
[24] T. H. Walter, L. Reven, E. Oldfield, *J. Phys. Chem.* **1989**, *93*, 1320–1326.
[25] R. Tycko, G. Dabbagh, G. B. M. Vaughan, P. A. Heiney, R. M. Strongin, M. A. Cichy, A. B. Smith, *J. Chem. Phys.* **1993**, *99*, 7554–7564.
[26] E. Mocellin, M. Ravera, R. A. Russell, T. Hynson, *J. Chem. Educ.* **1996**, *73*, A99–A102.
[27] W. F. Armarego, D. D. Perrin, *Purification of Laboratory Chemicals*, Butterworth Heinemann, New York, **1998**.
[28] A. Harada, Y. Hu, S. Yamamoto, S. Takahashi, *J. Chem. Soc. Dalton Trans.* **1988**, 729–732.
[29] S. Aime, M. Botta, R. Gobetto, A. Orlandi, *Magn. Reson. Chem.* **1990**, *28*, S52–S58.

Received: July 27, 2007